

Electronic Supplementary Information

Rhodium-cobalt alloy bimetallic towards liquid C1 molecules electrooxidation in alkaline media

Wei Zhong,^a Bo-Qiang Miao,^a Ming-Yao Wang,^a Yu Ding,^{*a} Dong-Sheng Li,^b Shi-Bin Yin,^c Xi-Fei Li^d
and Yu Chen^{*a}

^aKey Laboratory of Macromolecular Science of Shaanxi Province, Key Laboratory of Applied Surface and Colloid Chemistry (Ministry of Education), Shaanxi Key Laboratory for Advanced Energy Devices, Shaanxi Engineering Lab for Advanced Energy Technology, School of Materials Science and Engineering, Shaanxi Normal University, Xi'an 710062, PR China.

^b College of Materials and Chemical Engineering, Key Laboratory of Inorganic Nonmetallic Crystalline and Energy Conversion Materials, China Three Gorges University, Yichang, 443002, PR China

^cMOE Key Laboratory of New Processing Technology for Non-ferrous Metals and Materials, Guangxi Key Laboratory of Processing for Non-ferrous Metals and Featured Materials, Guangxi University, Nanning, Guangxi 530004, PR China.

^d Key Laboratory of Advanced Batteries Materials for Electric Vehicles of China Petroleum and Chemical Industry Federation, School of Materials Science and Engineering, Xi'an University of Technology, Xi'an 710048, PR China

**Corresponding Authors*

E-mail addresses: dingyu2527@gmail.com (Y. D.), ndchenyu@gmail.com (Y. C.)

Experimental

Reagents and chemicals

Rhodium(III) chloride trihydrate ($\text{RhCl}_3 \cdot 3\text{H}_2\text{O}$, $\geq 99.9\%$) was purchased from Jiu Gu New Material Co., Ltd. (Shanghai, China). Potassium hexacyanocobaltate(III) ($\text{K}_3[\text{Co}(\text{CN})_6]$, 99%) was received from Macklin Biochemical Co., Ltd. (Shanghai, China). Methanol (CH_3OH , $>99.5\%$), formaldehyde (HCHO , 37–40%), and hydrochloric acid (HCl , 36–38%) absolute was purchased from Sinopharm Chemical Reagent Co., Ltd. (Shanghai, China). Potassium hydroxide (KOH , $>85\%$) and potassium formate (HCOOK , $>99\%$) were purchased from Alfa Aesar. Commercial Rh nanoparticles (Rh C-NPs) electrocatalyst was bought from Sigma-Aldrich Co., Ltd. (Shanghai, China). Commercial Pt nanoparticles (Pt C-NPs) and commercial Pd nanoparticles (Pd C-NPs) electrocatalyst were obtained from Johnson Matthey Corporation. Ultrapure water (resistance $>18.2 \text{ M}\Omega \cdot \text{cm}^{-1}$) was used in all of the experiments.

Synthesis of Rh-Co ABM

Typically, 5 mL of the mixture solution containing RhCl_3 (5.0 mg) and $\text{K}_3[\text{Co}(\text{CN})_6]$ (4.0 mg) was transferred into a high-pressure reaction kettle at 220°C for 12 h to form the Rh-Co alloy. After reaction, the sample was washed by concentrated hydrochloric acid and water several times to remove the unalloyed Co and vacuum drying at 60°C for 5 h to obtain Rh-Co ABM. Additionally, the experimental details about physical characterization, electrochemical measurements, and density functional theory were provided in Supporting Information.

Physical characterization

The morphology, structure, and composition of sample were investigated using scanning electron microscope (SEM, SU-8020) and transmission electron microscopy (TEM, JEM-2800) with high-resolution TEM (HRTEM) and energy dispersive X-ray spectroscopy maps function (EDX). Surface information/crystallographic texture were conducted through X-ray diffraction (XRD, DX-2700) with $\text{Cu K}\alpha$ radiation source at room temperature. The electronic and surficial

information of sample were analyzed by X-ray photoelectron spectroscopy (XPS, AXIS ULTRA). Atomic force microscopy (AFM, Dimension ICON,) was used to measuring the thickness of samples. Herein, the XRD analysis on the degree of alloying (X) in the Rh-Co ABM catalysts can be achieved using Vegard's law ($X = \frac{a_{\text{exp}} - a_0}{a_{\text{alloy}} - a_0}$), where a_{exp} is the experimental value of lattice parameter for binary Rh-Co ABM crystals, a_{alloy} is the lattice parameter assuming that all Co is alloyed, and a_0 is the lattice parameter of pure Rh. Herein the a_{alloy} value can be determined from the following expression.¹ The Rh (111) peak was chosen to evaluate lattice parameter of Rh. The precise peak positions (θ_{max}) were obtained through curve fitting, and the lattice parameter (a) was calculated using the following equation as shown ($a = \frac{\sqrt{h^2 + k^2 + l^2} \lambda}{2 \sin \theta}$).²

Electrochemical measurements

All electrochemical were carried out on a CHI-660 electrochemical workstation at 30°C. In a three-electrode system, a saturated calomel electrode (SCE) was used as a reference electrode, a carbon rod served as a counter electrode, and an electrocatalyst-modified glassy carbone (diameter: 3 mm) was used as a working electrode. In our experiment, the SCE is protected by Luggin capillary with KCl solution, which can effectively prevent the permeation of OH⁻ ion and consequently avoid the damage of SCE. Therefore, the reference electrode in our experiment is stable under alkaline conditions. All the potentials reported in this work had been referenced to a relative hydrogen electrode (RHE) using equation ($E_{\text{RHE}} = E_{\text{SCE}} + 0.0591 \text{ pH} + 0.242$). The electrocatalyst ink was obtained by dispersing 4 mg electrocatalyst in 2 mL mixed solution of isopropanol and water. Then, 4 μL of the electrocatalyst ink was loaded onto the glassy carbon electrode surface and dried at room temperature. Finally, 4 μL of Nafion solution (5 wt%) was coated on the working electrode surface, after drying at room temperature, the working electrode was obtained. The electrocatalyst loading mass density on working electrode was 0.11 mg cm⁻². The calculation of ECSAs was completed by integrating the area of H desorption on metal surface according to Equation (ECSA = $Q/(C \times m)$), where Q was the Coulombic charge of the H desorption peak area; m was the mass of Rh on the electrode surface; and C was the hydrogen adsorption constant, for polycrystalline Rh, C was 220 $\mu\text{C cm}^{-2}$.

DFT calculations

For all structural optimization and energy calculation, all the spin-polarized DFT calculations were used Vienna Ab-Initio Simulation Package (VASP).^{3 4} The electronic exchange interaction were described by Generalized gradient approximation (GGA) function developed by Perdew, Burke and Ernzerhof (PBE).⁵ 2×3 supercell structures were employed to simulate the RhCo (111) and Rh (111) surfaces. All the calculation in our work was applied the plane wave cutoff energy of 450 eV, the energy convergence criterion of 1×10^{-5} eV, and optimized the structure until the force per atom is less than $0.05 \text{ eV}\text{\AA}^{-1}$ to improve the accuracy. Monkhorst-Pack ⁶ scheme based on Gamma was used to set a $3 \times 3 \times 1$ grid to calculate Brillouin zone integrals for structural relaxation in k-point option. The adsorption energy (E_{ads}) of the CO molecule on the surface was calculated by the following equation: $E_{\text{ads}} = E_{\text{total}} - E_{\text{S}} - E_{\text{CO}}$

where E_{total} , E_{S} , and E_{CO} are the total energies of the complex of adsorbate-substrate (total), the substrate (S), and the adsorbate (CO) in their equilibrium gas-phase configuration, respectively. To derive the theoretical catalytic activity of RhCo(111) and Rh(111) for methanol oxidation, we used the following formula to calculate the free energy change of the electron transfer of the reaction:

$$\Delta G = \Delta E + \Delta \text{ZPE} - T\Delta S$$

ΔE , ΔZPE and $T\Delta S$ in the above equation represent the change in electron energy, the zero-point energy correction and the influence of entropy energy, respectively. T is the room temperature of standard atmospheric pressure (298.15 K).

References

1. C.-T. Hsieh, P.-Y. Yu, D.-Y. Tzou, J.-P. Hsu and Y.-R. Chiu, *J. Electroanal. Chem.*, 2016, **761**, 28-36.
2. K.-S. Lee, T.-Y. Jeon, S. J. Yoo, I.-S. Park, Y.-H. Cho, S. H. Kang, K. H. Choi and Y.-E. Sung, *Appl. Catal. B-Environ.*, 2011, **102**, 334-342.
3. G. Kresse and J. Furthmüller, *Phys. Rev. B*, 1996, **54**, 11169-11186.
4. S. Goedecker, M. Teter and J. Hutter, *Phys. Rev. B*, 1996, **54**, 1703-1710.
5. J. P. Perdew, K. Burke and M. Ernzerhof, *Phys. Rev. Lett.*, 1996, **77**, 3865-3868.
6. H. J. Monkhorst and J. D. Pack, *Phys. Rev. B*, 1976, **13**, 5188-5192.

Figures

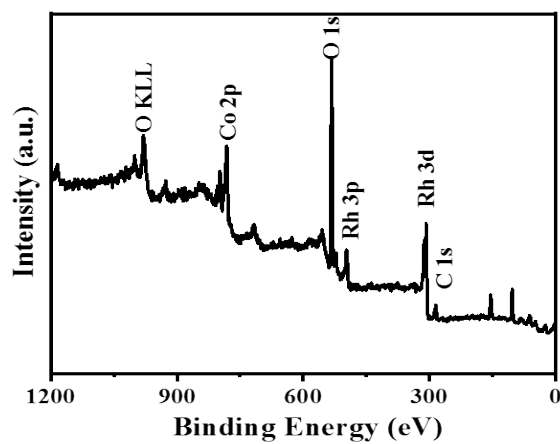


Fig. S1. XPS broad spectrum of Rh-Co ABM.

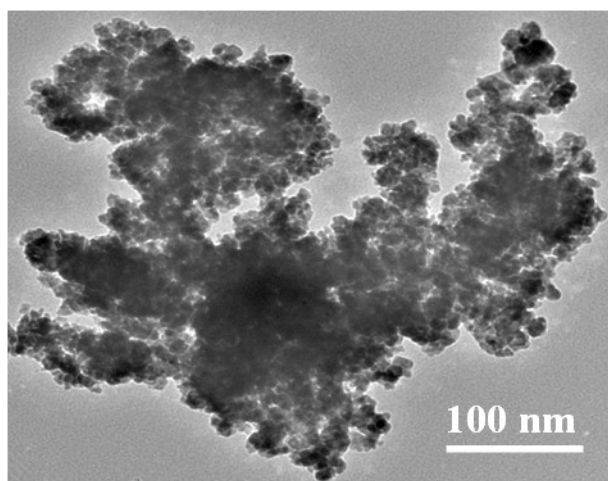


Fig. S2. TEM image of Rh C-NPs.

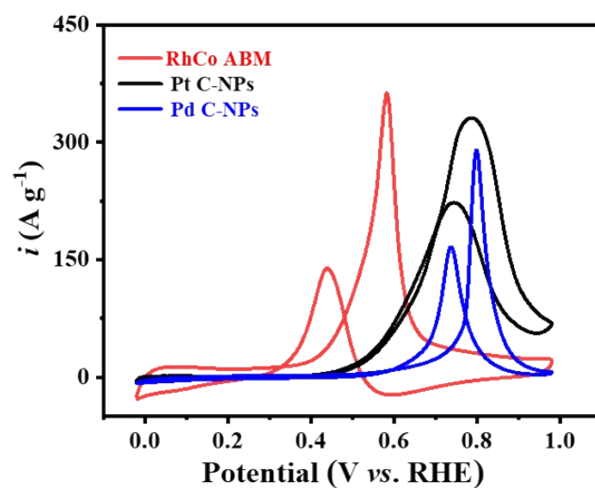


Fig. S3. Rh-mass normalized CV curves of Rh-Co ABM and Pt C-NPs and Pd C-NPs in Ar-saturated 1.0 M CH₃OH + 1.0 M KOH electrolyte at 50 mV s⁻¹.

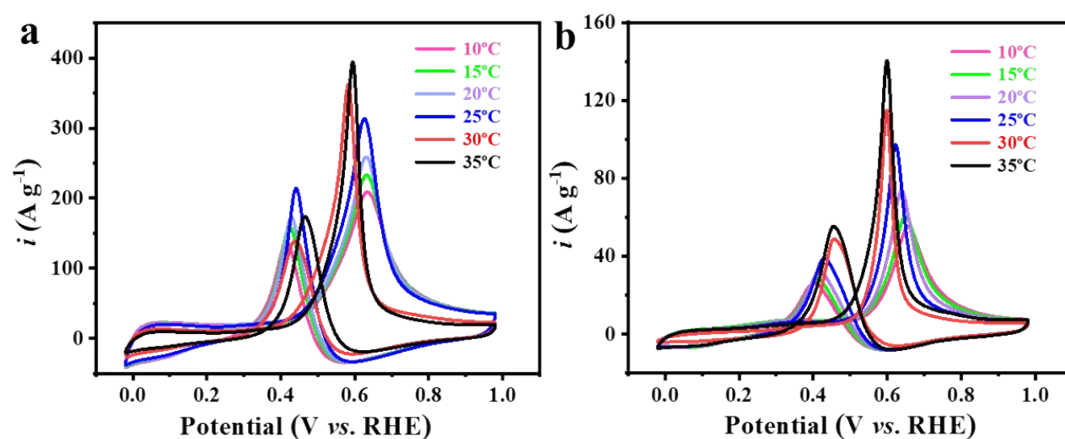


Fig. S4. Rh-metal normalized CV curves of (A) Rh-Co ABM and (B) Rh C-NPs in Ar-saturated of 1.0 M CH_3OH + 1.0 M KOH electrolyte at 50 mV s^{-1} at different temperatures of 10°C , 15°C , 20°C , 25°C , 30°C , and 35°C , respectively.

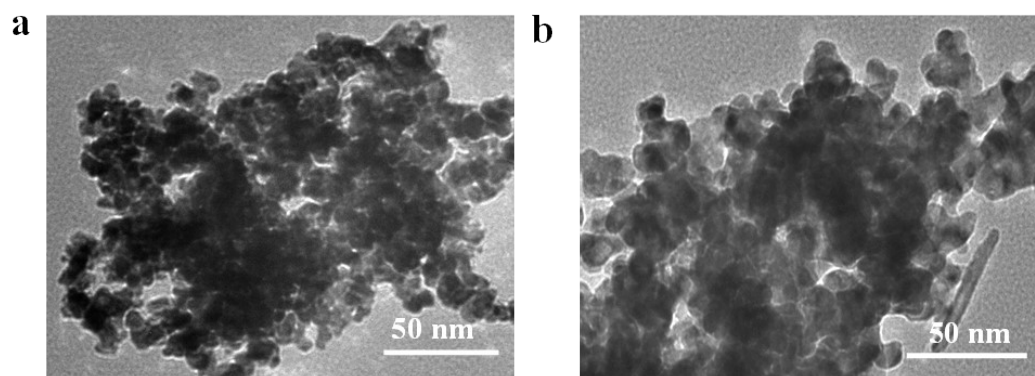


Fig. S5. TEM images of (a) Pt C-NPs and (b) Pd C-NPs.

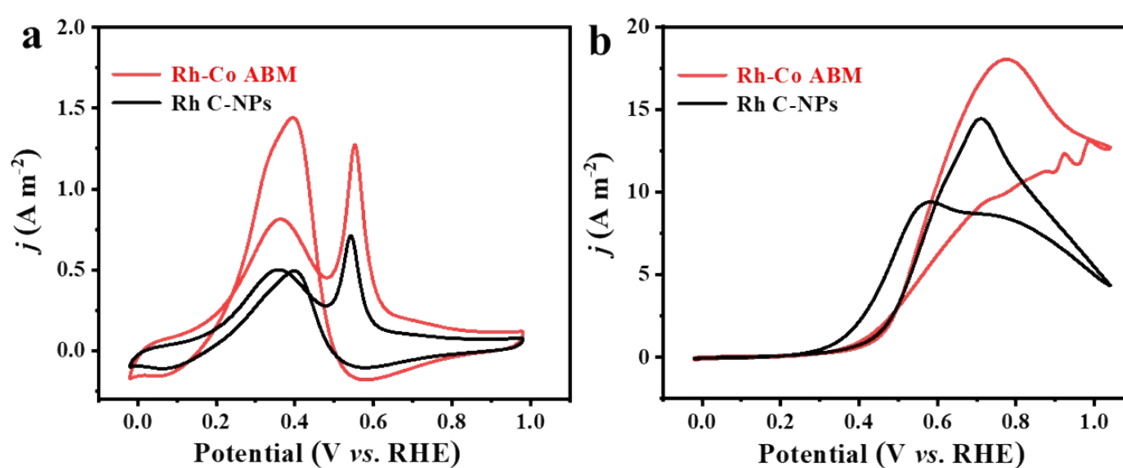


Fig. S6. ECSA normalized CV curves of Rh-Co ABM and Rh C-NPs in Ar-saturated (A) 1.0 M HCOOK + 1 M KOH electrolyte and (B) 1.0 M HCHO + 1.0 M KOH electrolyte at 50 mV s^{-1} .

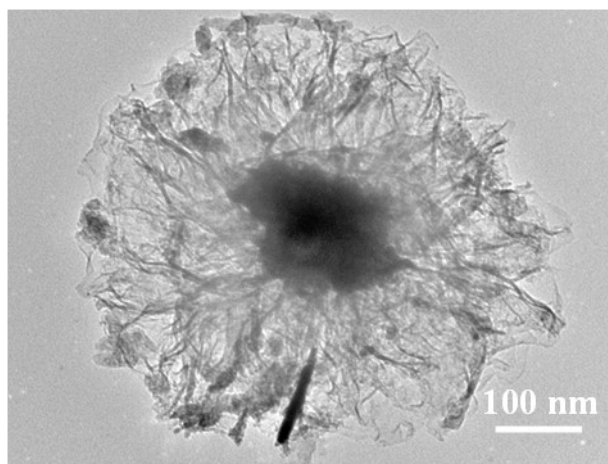


Fig. S7. TEM image of Rh-Co ABM after chronoamperometry test for MOR.